Title	A multi-mode flexible power point tracking algorithm for photovoltaic power plants
Author(s)	Dehghani Tafti, Hossein; Townsend, Christopher David; Konstantinou, Georgios; Pou, Josep
Citation	Dehghani Tafti, H., Townsend, C. D., Konstantinou, G., & Pou, J. A Multi-Mode Flexible Power Point Tracking Algorithm for Photovoltaic Power Plants. IEEE Transactions on Power Electronics, 1-1. doi:10.1109/TPEL.2018.2883320
Date	2018
URL	http://hdl.handle.net/10220/46909
Rights	© 2018 Institute of Electrical and Electronics Engineers (IEEE). This is the author created version of a work that has been peer reviewed and accepted for publication by IEEE Transactions on Power Electronics, Institute of Electrical and Electronics Engineers (IEEE). It incorporates referee's comments but changes resulting from the publishing process, such as copyediting, structural formatting, may not be reflected in this document. The published version is available at: [http://dx.doi.org/10.1109/TPEL.2018.2883320].

A Multi-Mode Flexible Power Point Tracking Algorithm for Photovoltaic Power Plants

Hossein Dehghani Tafti, *Member, IEEE,* Christopher D. Townsend, *Member, IEEE,*
Georgios Konstantinou, *Senior Member, IEEE, and* Josep Pou, *Fellow, IEEE,*

Abstract—**Flexible power point tracking (FPPT) is the control of active power generated by grid-connected photovoltaic power plants (GCPVPPs) to provide grid-support functionality. An FPPT algorithm for the reduction of the extracted power from photovoltaic (PV) strings during voltage sags was previously proposed by the authors. An advantage of this algorithm, compared to conventional FPPT algorithms, was its fast dynamics facilitated by use of a simple PI controller that dynamically modifies the PV voltage reference. The previously proposed scheme could only be employed for the short-duration in which the power system experiences a voltage sag. A novel modification to this algorithm with multi-mode operation is introduced in this letter, which provides FPPT capability for continuous operation of GCPVPPs. Unlike the previous algorithm, which was able to only move the operation point to the right-side of MPP, the proposed algorithm in this letter is able to move the operation point to both right- and left-sides of the MPP that provides the flexibility to operate in the optimum operation region for both single- and two-stage GCPVPPs. Experimental results are provided to demonstrate the performance of the proposed algorithm under dynamic irradiance conditions.**

Index Terms – **Flexible power point tracking, photovoltaic systems, active power control, constant power generation, two-stage photovoltaic power plants.**

I. INTRODUCTION

Flexible power point tracking (FPPT) algorithms have been developed in order to provide frequency support and low-voltage ride-through (LVRT) capabilities for grid-connected photovoltaic power plants (GCPVPPs) [1]. The principles of FPPT are demonstrated in Fig. 1. Unlike maximum power point tracking (MPPT) algorithms, which always extract the available maximum power (p_{mpp}) from the PV strings, by operating at the maximum power point (MPP) in Fig. 1(a), the FPPT algorithms regulate the PV power (p_{pv}) to a power reference (p_{fpp}), received from an upper level control system, by operating the PV strings at points A or B in Fig. 1(a). Furthermore, by applying FPPT algorithms, the injected active power to the grid can be reduced during grid voltage sags, in order to provide reactive power injection capability based on the grid requirements. Additionally, power ramp rate control can be attained by applying FPPT algorithms in GCPVPPs [2]. Various FPPT algorithms are introduced in the literature with various advantages and disadvantages [3], [4]. It is noted that GCPVPPs with FPPT functionality are required to be over-sized, compared to the GCPVPPs with MPPT functionality, but with the added benefits of grid support functionality.

Several FPPT algorithms for the operation of two-stage GCPVPPs (those with integrated dc-dc converters) during voltage sags have been proposed in [5]–[7]. The injection of reactive power to the grid, based on the grid code require-ments, may impose a reduction in the injected active power to
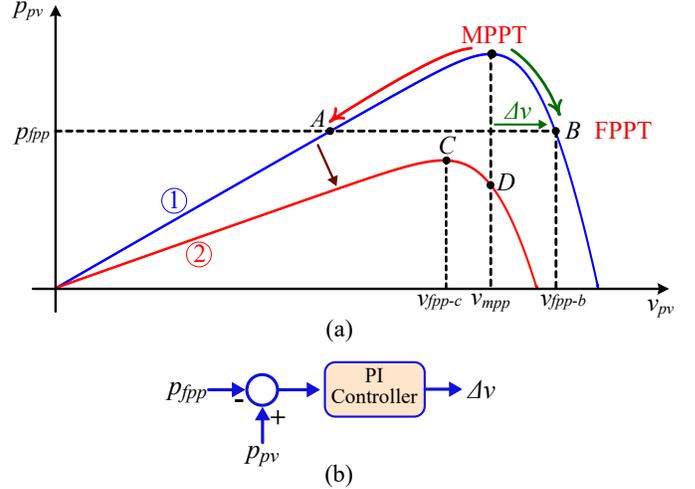

Fig. 1. Principles of flexible power point tracking in GCPVPPs: (a) Power-voltage curve under various operation conditions, and (b) algorithm for the calculation of Δv.

avoid exceeding the maximum current rating of the inverter. In these proposed algorithms, the MPPT algorithm stops its operation during grid voltage sags, while the control platform records the last calculated voltage reference associated with the MPP, prior to the detection of the voltage sag. To regulate the PV power to the required power reference during the voltage sag, the operation point of the PV strings is moved to the right-side of the MPP, by adding an additional voltage Δv to the last recorded MPP voltage, as shown in Fig. 1(a). The value of Δv is calculated by a proportional-integral (PI) controller, as shown in Fig. 1(b). The input of the PI controller is the error between the PV power p_{pv} and power reference p_{fpp} [6], or the error between the dc-link voltage and its reference [5], [7].

The main advantage of the algorithms of [5]–[7], compared to other available FPPT algorithms in the literature [3], [4], is fast dynamic performance. This is achieved with the use of a PI controller that adaptively calculates the PV voltage reference. In conventional FPPT algorithms, like those based on the perturb & observe (P&O) algorithm, a constant voltage-step with low-frequency calculation bandwidth (e.g. $1-20\,\text{Hz}$ in practical applications) is usually applied. In this case, fast dynamics can be attained by using a relatively large voltage-step. However, large voltage-step values result in large power oscillations at steady-state.

In the algorithms of [5]–[7], it is assumed that the duration of the grid voltage sag is relatively short ($\leq 150\,\text{ms}$) and that there is no significant change in environmental condi-tions (irradiance, temperature, etc.) during this period, which means that the MPP voltage remains constant. The following

example demonstrates why these algorithms cannot ensure the extraction of constant power from PV strings over long time periods, in which prevailing environmental conditions change. In Fig. 1, initially, the power-voltage (P-V) curve of the PV panel is curve ①. The PV operates at point B, achieved by adding Δv to the last recorded MPP voltage (v_{mpp}) before the occurrence of the voltage sag. Due to sudden environmental changes, the P-V curve changes to curve ②. In this condition, the appropriate FPPT operation point is C, because the maximum available PV power is smaller than p_{fpp}. However, the algorithms of [5]–[7] cannot track the voltage of point C. This is because the MPP voltage is assumed to be constant at v_{mpp} and the error between p_{pv} and p_{fpp} is positive, which results in a large positive Δv in the output of the PI controller, shown in Fig. 1(b). Accordingly, the algorithm will keep the operation point beyond the open circuit voltage of the PV string. Therefore, these algorithms cannot ensure the continuous FPPT operation of GCPVPPs.

To extend the applicability of these algorithms for continuous operation, a multi-mode-based FPPT is proposed in this letter. In one operation mode, a conventional MPPT algorithm is performed to increase the PV power, while in the second operation mode, a PI controller is implemented to reduce the PV power towards its desired value. The proposed algorithm is also applicable for both single- and two-stage GCPVPPs, because it is able to move the operation point to the right or left-side of the MPP.

II. PROPOSED MULTI-MODE FPPT ALGORITHM

The control diagram of the proposed multi-mode FPPT algorithm is shown in Fig. 2. There are two operation modes, depending on the relation between the PV power p_{pv} and power reference p_{fpp}, as follows:

Mode I ($p_{fpp} \leq p_{pv}$): In this mode, the PV power should be decreased. To decrease the power, the MPPT algorithm ceases its operation and the last recorded MPP voltage reference ($v_{fpp\text{-}old}$) is used, as illustrated in Fig. 2(a). For the operation in the left-side of MPP, the reduction of the PV power is achieved by substituting the calculated Δv from $v_{fpp\text{-}old}$ ($v_{fpp} = v_{fpp\text{-}old} - \Delta v$). As shown in Fig. 1(b), Δv is calculated using a PI controller. The input of this PI controller is the error between the PV power p_{pv} and power reference p_{fpp}, which is calculated on a high-frequency calculation bandwidth (e.g. calculation bandwidth of the control platform). Furthermore, for a relatively large error value, Δv becomes relatively large, which moves the operation point towards its desired point in a short time interval. This feature results in fast dynamic performance of the proposed algorithm. If the PV operation point is close to its reference point, the error is small, which contributes to a relatively small value for Δv. Consequently, only small power oscillations around the operating point are obtained during steady-state. It should be mentioned that PV voltage is adjusted with a high-frequency calculation bandwidth (the calculation frequency bandwidth of the controller platform, e.g. 100 kHz) in the proposed algorithm, which results in fast dynamics compared to conventional FPPT algorithms with relatively low calculation bandwidth.
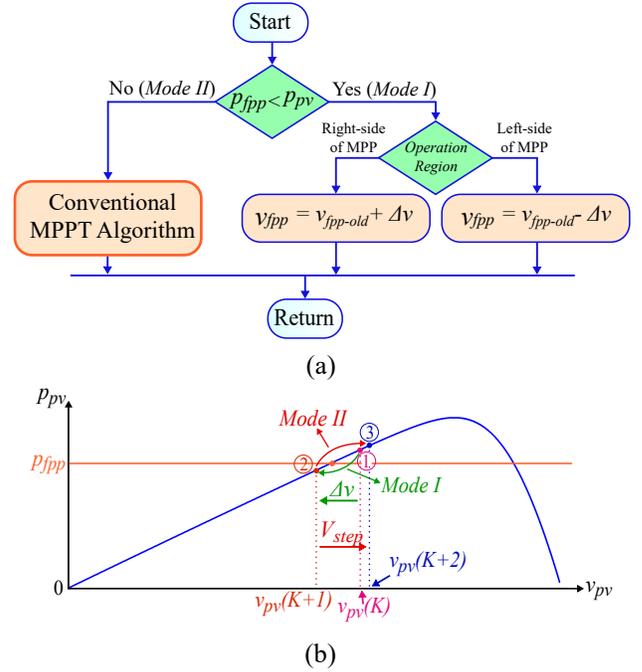

Fig. 2. Proposed multi-mode FPPT algorithm: (a) Control diagram of the algorithm, and (b) demonstration of the multi-mode operation.

This mode is demonstrated in Fig. 2(b). At $t = KT$, where K is the number of the calculation step and T is the calculation time-step, the PV voltage is $v_{pv}(K)$ at point ①. At this point, p_{pv} is larger than p_{fpp}, hence the proposed algorithm reduces the PV voltage by subtracting its previous value by Δv, as discussed above. As a result of the reduction of the PV voltage, the operation point moves to point ②, which produces less power, compared to p_{fpp}.

Mode II ($p_{fpp} > p_{pv}$): In this mode, the algorithm increases the PV power by activating the MPPT algorithm, as shown in Fig. 2. Any conventional MPPT algorithm can be deployed. In this study, P&O MPPT algorithm is implemented. It is based on a step-change of the PV voltage (V_{step}) in each calculation-step and determination of the direction of the next voltage change, based on the PV power change. The parameter Δv is not added to the voltage reference calculated by the MPPT algorithm in this condition. Hence, the MPPT algorithm increases the PV power towards p_{fpp}. This operation is shown in Fig. 2(b). At $t = (k + 1)T$, $v_{pv} = v_{pv}(K + 1)$ and the operation point is at ② with $p_{pv} < p_{fpp}$. Accordingly, the proposed algorithm operates in *Mode II* and the MPPT algorithm increases the PV power by adding a voltage-step V_{step} to the PV reference voltage. As a result of this action, the operation point moves to ③, with higher power than p_{fpp}, as shown in Fig. 2(b). It is noted that implementing an MPPT algorithm in *Mode II* does not mean that the operation point is moved to the maximum power point. It simply means that the PV power is increased by moving the operation point towards the maximum power point (point ③).

The multi-mode operation feature of the proposed algorithm facilitates continuous operation capability. Unlike the algorithms of [5]–[7], the MPPT operation is not ceased during the FPPT operation and instead, it is implemented as one of the operation modes. If the PV power becomes smaller than
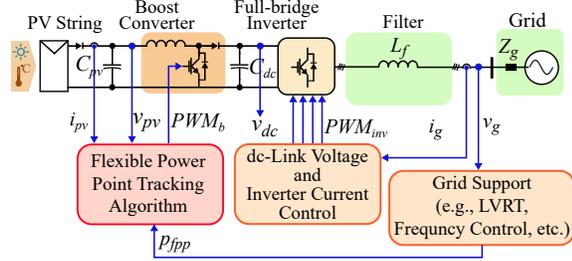
Fig. 3. Circuit diagram of experimental verification on a down-scaled two-stage GCPVPP.

p_{fpp}, due to environmental changes or variations in p_{fpp} from an upper level controller, *Mode II* is activated, which increases the PV power via the MPPT operation.

The proposed algorithm is also able to move the operation point to the right-side of the MPP. The only difference is that during *Mode I* operation, the value Δv should be added to $v_{fpp\text{-}old}$, instead of being subtracted from it. It should be mentioned that the selection of the optimized operation regions should be performed by a higher level controller and is not the main focus of this study. The FPPT operation in the right-side of MPP provides faster dynamic performance compared to the left-side of MPP, because a small change in the voltage results in a large change of power. On the other hand, the operation in the right-side of MPP results in larger power oscillations compared to the left-side of MPP. This should be considered in the design of the PI control parameters.

III. EXPERIMENTAL EVALUATION

The performance of the proposed multi-mode FPPT algorithm is evaluated on a scaled-down two-stage GCPVPP. The circuit diagram of the system is shown in Fig. 3. It consists of a dc-dc boost converter with FPPT functionality and a grid-connected inverter, which regulates the dc-link voltage to its desired value and complies with grid code requirements. The power reference p_{fpp} is calculated with the controller of the grid-connected inverter. The PV panel is simulated using the Chroma 62000H-S solar array simulator. The maximum power of the PV panel at irradiance of $Irr = 1000\,\mathrm{W/m^2}$ and temperature of $T = 25\,^\circ\mathrm{C}$ is $p_{mpp} = 800\,\mathrm{W}$ ($v_{mpp} = 110\,\mathrm{V}$ and $i_{mpp} = 7.3\,\mathrm{A}$). The grid voltage ($v_{rms} = 70\,\mathrm{V}$) is synthesized using a Cinergia grid emulator. The dc-ac inverter and dc-dc converters are implemented using Imperix full-bridge modules. The dc-link voltage is $170\,\mathrm{V}$ and the controller is implemented on the Boombox control platform. Two case studies with the movement of operation point to the right- and left-side of the MPP are performed under fast irradiance changes.

In order to verify the performance of the algorithm proposed in this paper (referred to as *Method 1*), the results are compared with the algorithm of [3], [8], [9] (referred to as *Method* 2). In *Method 2*, the PV voltage reference is calculated directly via an FPPT algorithm, which is based on the modification of the P&O algorithm. The same voltage-step ($V_{step} = 1\,\mathrm{V}$) and calculation time-step for MPPT and FPPT algorithms ($T_{step} = 0.2\,\mathrm{s}$. i.e., the calculation bandwidth of the FPPT algorithm is $5\,\mathrm{Hz}$) are considered in all of the case studies to provide a fair comparison. To obtain a numerical comparison between the performance of these algorithms, two
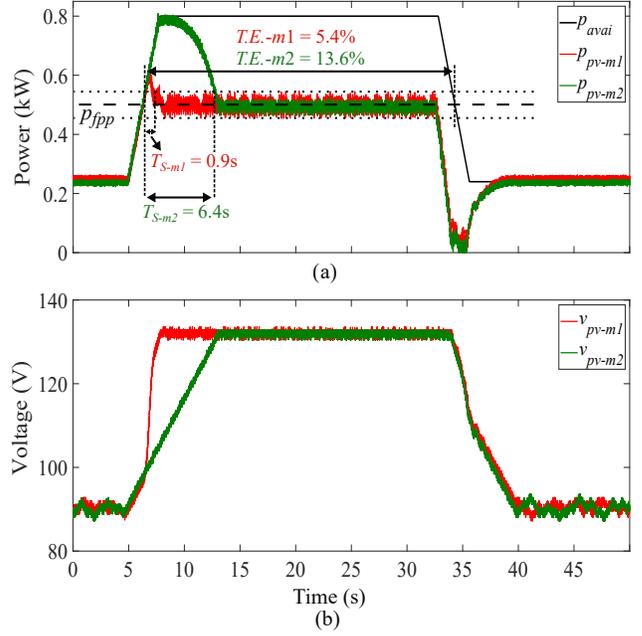

Fig. 4. Performance of the proposed algorithm under fast environmental changes with the movement of the operation point to the right-side of MPP (*Case I*): (a) PV power and (b) PV voltage.

parameters are analyzed in the experimental results: 1) settling time of the controller, which is the time elapsed between when the available PV power is equal to or larger than p_{fpp} to the time that the PV power enters and remains within a 5% error band of its reference value; and 2) average tracking error in percentage of the total energy yield ($T.E.$), which is calculated as [2]:

$$T.E. = \frac{\int |p_{pv} - p_{fpp}|}{\int |p_{pv}|} \times 100. \tag{1}$$

Case I: The performance of the proposed algorithm for the movement of the operation point to the right-side of MPP is evaluated in this case study and results are presented in Fig. 4. Initially, the irradiance is $Irr = 300\,\mathrm{W/m^2}$ and the maximum available PV power is $p_{avai} = 240\,\mathrm{W}$. From $t = 5\,\mathrm{s}$ to $t = 7.8\,\mathrm{s}$, the irradiance increases linearly from $300\,\mathrm{W/m^2}$ to $1000\,\mathrm{W/m^2}$. Correspondingly, the available PV power rises from $240\,\mathrm{W}$ to $800\,\mathrm{W}$. Subsequently, the irradiance remains constant at $1000\,\mathrm{W/m^2}$ for a duration of $25\,\mathrm{s}$ until $t = 32.8\,\mathrm{s}$, in which it starts to reduce to $300\,\mathrm{W/m^2}$ for a transient period of $2.8\,\mathrm{s}$.

The maximum available PV power under this condition is shown in Fig. 4(a). The power reference for the FPPT algorithm (p_{fpp}) is $500\,\mathrm{W}$ in this case study. The PV power curves under the implementation of the proposed algorithm ($p_{pv\text{-}m1}$) and *Method 2* ($p_{pv\text{-}m2}$) are illustrated in Fig. 4(a). If the available PV power is smaller than p_{fpp}, the algorithms extract the maximum power from the PV strings. The PV power overshoot by the implementation of the proposed algorithm is relatively small, while the overshoot under *Method 2* is relatively large. The superior performance of the proposed algorithm is achieved because the PV voltage is adaptively calculated through the PI controller. Furthermore, the FPPT algorithm in *Method 2* is updated every $0.2\,\mathrm{s}$ (FPPT calculation
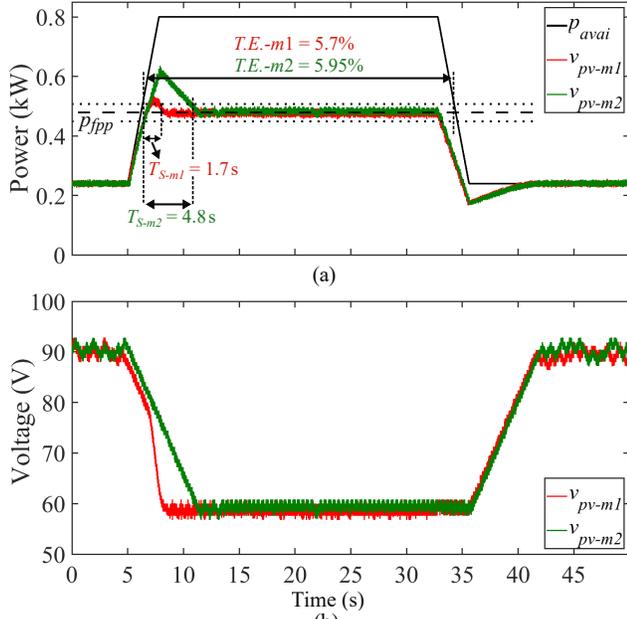
Fig. 5. Performance of the proposed algorithm under fast environmental changes with the movement of the operation point to the left-side of MPP (*Case II*): (a) PV power and (b) PV voltage.

time-step), as the lower limit for the time-step is determined by acceptable oscillation in steady-state conditions, while the PI controller in the proposed algorithm adjusts the PV voltage reference every $10\,\mu$s (the controller platform calculation time-step). The settling time of the proposed algorithm ($T_{S\text{-}m1}$) is $0.9\,s$, while it is equal to $T_{S\text{-}m2} = 6.4\,s$ for *Method* 2. The tracking error ($T.E.$) is calculated over the time interval that $p_{avai} > p_{fpp}$ (in this case between $t = 6.3\,s$ and $t = 34.3\,s$). It is seen that the tracking error of the proposed algorithm (*Method 1*) is smaller than *Method 2* by 8.2%. These two parameters verify the faster dynamics of the proposed algorithm under fast increments of irradiance, compared to the conventional algorithm. The PV voltage curves for both of the algorithms are shown in Fig. 4(b). The PV voltage is increased during the FPPT operation, which implies the operation in the right-side of the MPP.

Both of the algorithms have similar performance under a fast reduction of irradiance, because the proposed algorithm mostly operates at *Mode II* in this condition. Since the same MPPT algorithm (P&O) is implemented in both methods, similar performance is achieved. It should be noted that the performance under fast increase of irradiance is more important and challenging, compared to the fast decrease of irradiance. This is because the excess of energy extracted from the PV panels under irradiance increase can be stored in the dc-link capacitor and increase its voltage beyond the nominal limit.

Case II: The performance of the proposed multi-mode FPPT algorithm in the left-side of the MPP is compared with the conventional algorithm and results are shown in Fig. 5. Similar test conditions as *Case I* are implemented in this case study. The PV voltage during FPPT operation is decreased, which implies operating on the left-side of the MPP. The overshoot of the PV power under fast irradiance

increase is smaller in the proposed algorithm, compared to the conventional algorithm. Consequently, the settling time of the proposed algorithm is improved compared to the conventional algorithm, while the tracking error remains equal for both of the algorithms, as shown in Fig. 5(a). This confirms the fast dynamic performance of the proposed algorithm in both left- and right-side of MPP.

IV. CONCLUSION

A multi-mode FPPT algorithm for GCPVPPs has been introduced in this letter. The operation mode of the proposed algorithm is selected based on comparing the PV power with the desired power reference. If the PV power is larger than the power reference, an additional value Δv is added to the voltage of the MPP to facilitate operation on the right-side of the MPP. Similarly, Δv is subtracted from the voltage of the MPP to facilitate operation on the left-side of the MPP. Since the additional voltage value is calculated based on the error between the PV power and the power reference, fast dynamics are obtained. If the PV power is smaller than its reference value, a conventional MPPT algorithm is applied to increase the PV power by moving its operation point towards the MPP. The main advantage of the proposed algorithm, compared to the conventional algorithms, is its fast dynamics and low power oscillations during the steady-state. Furthermore, it is able to move the operation point to the right- or left-side of MPP, which makes it applicable to both single- and two-stage GCPVPPs to operate in the optimum region. Experimental results illustrate the fast dynamic performance of the proposed algorithm under fast environmental changes.

REFERENCES

[1] Energinet.dk, "Technical regulation 3.2.2 for PV power plants with a power output above 11 kW," *Energinet.dk, Errits, Denmark, Document No.: 14/17997-39, Tech. Rep.*, 2015.

[2] Y. Yang, F. Blaabjerg, and Z. Zou, "Benchmarking of grid fault modes in single-phase grid-connected photovoltaic systems," *IEEE Trans. Ind. App.*, vol. 49, no. 5, pp. 2167–2176, Sep. 2013.

[3] H. D. Tafti, A. I. Maswood, G. Konstantinou, J. Pou, and F. Blaabjerg, "A general constant power generation algorithm for photovoltaic systems," *IEEE Trans. Power Electron.*, vol. 33, no. 5, pp. 4088–4101, May 2018.

[4] H. D. Tafti, A. Sangwongwanich, Y. Yang, J. Pou, G. Konstantinou, and F. Blaabjerg, "An adaptive control scheme for flexible power point tracking in photovoltaic systems," *IEEE Trans. Power Electron.*, vol. PP, pp. 1–1, 2018.

[5] H. D. Tafti, A. Maswood, G. Konstantinou, J. Pou, K. Kandasamy, Z. Lim, and G. H. P. Ooi, "Study on the low-voltage ride-thorough capability of photovoltaic grid-connected neutral-point-clamped inverters with active/reactive power injection," *IET Renewable Power Generation*, vol. 11, no. 8, pp. 1182–1190, Jul. 2017.

[6] H. D. Tafti, A. I. Maswood, G. Konstantinou, J. Pou, and P. Acuna, "Active/reactive power control of photovoltaic grid-tied inverters with peak current limitation and zero active power oscillation during unbalanced voltage sags," *IET Power Electron.*, vol. 11, no. 6, pp. 1066–1073, May 2018.

[7] M. Mirhosseini, J. Pou, and V. G. Agelidis, "Single- and two-stage inverter-based grid-connected photovoltaic power plants with ride-through capability under grid faults," *IEEE Trans. Sustain. Energy*, vol. 6, no. 3, pp. 1150–1159, Jul. 2015.

[8] A. Sangwongwanich, Y. Yang, and F. Blaabjerg, "High-performance constant power generation in grid-connected pv systems," *IEEE Trans. Power Electron.*, vol. 31, no. 3, pp. 1822–1825, Mar. 2016.

[9] H. D. Tafti, A. Sangwongwanich, Y. Yang, G. Konstantinou, J. Pou, and F. Blaabjerg, "A general algorithm for flexible active power control of photovoltaic systems," in *Proc. IEEE Applied Power Electron. Conf. and Exposition (APEC)*, pp. 1115–1121, Mar. 2018.